Desalination and Water Treatment
www.deswater.com

doi: 10.5004/dwt.2017.20847

78 (2017) 292–299
June

Thermodynamic and kinetic studies of adsorptive removal of toluidine blue by activated carbon from olive pit

Mohammad Sadiq[a,*], Mashooq Khan[a,b], Razia Aman[a], Saima Sadiq[c], M. Sohail Ahmad[a], Muhammad Ali[a], Rahmat Ali[d]

[a]*Department of Chemistry, University of Malakand, Chakdara 18800, Pakistan, emails: sadiq@uom.edu.pk, mohammad_sadiq26@yahoo.com (M. Sadiq), razia.aman@yahoo.com (R. Aman), sohail850@gmail.com (M. Sohail Ahmad), muhammadali041988@yahoo.com (M. Ali)*
[b]*Department of Chemistry, Beijing Key Laboratory of Microanalytical Methods and Instrumentation, Tsinghua University, Beijing 100084, China, emails: mashooq_khan@yahoo.com, khan1985@mail.tsinghua.edu.cn*
[c]*School of Applied Chemical Engineering, Kyungpook National University, Daegu, Korea, email: saimasadiq1978@yahoo.com*
[d]*Department of Chemistry, National Center of Excellence in Physical Chemistry, University of Peshawar, Peshawar, Pakistan, email: rahmat_chemistpk@yahoo.com*

Received 23 November 2016; Accepted 19 April 2017

ABSTRACT

Activated carbon from olive pit (ACop) was prepared by H_3PO_4 and KOH activation followed by carbonization at 280°C. The ACop was characterized with physical techniques such as scanning electron microscopy (SEM), X-ray diffraction, Fourier transform infrared spectroscopy, Brunauer–Emmett–Teller (BET) surface area and pore size analyzer. The SEM images reveal porous nature of ACop; BET surface area and total pore volume of ACop were 1,209 m^2/g and 0.78 cm^3/g, respectively. The adsorption capability of ACop was tested for the removal of toluidine blue (TB) from aqueous solution in a batch type and fixed bed column reactor at experimental conditions such as temperature, adsorbent dosage, time, pH and initial dye concentrations. Batch studies show that the adsorption of TB on ACop proceeds through pseudo-second-order kinetics and follow Temkin adsorption isotherm at optimal reaction conditions. Fixed bed column studies revealed the industrial applicability of ACop for TB removal from industrial effluent. Thus, ACop can be a suitable adsorbent for the removal of TB from aqueous medium.

Keywords: Olive pit; Phosphoric acid; Adsorption; Toluidine blue

1. Introduction

Dyes have the complex chemical architecture with aromatic skeleton. On the basis of chemical structure, six classes of dyes exist such as sulfur, azo, indigoid, anthraquinone, triphenyl methane and phthalocyanine derivatives [1]. These have been used in various industries, such as paper, textiles, cosmetics, food, rubber, pulp and lather, to color their products [2]. Dyes were also used in paper printing, colored photography and as additives in petroleum products [3]. In fact, global productions of organic dyes are 450,000 t/year and approximately 15% of these dyes lost in wastewater [4], so it has become a permanent part of the industrial wastewater. Due to complex structure, dyes have high stability and cannot be removed easily from wastewater [5]. In textile industries about 10%–60% losses of reactive dyes were recorded in wastewater which was released to the environment [6]. The existence of these dyes not only cause the unwanted color of water but also prevent the entrance of sun light into water which stop photosynthesis in aqueous plants and so the growth of aquatic biota [4,6,7]. Furthermore, the toxicity of dyes includes carcinogenicity, cytotoxicity, hepatotoxicity, microbial toxicity, mutagenicity, neurotoxicity and photodynamic toxicity [8,9].

* Corresponding author.

Thus, it is quite important to remove these chemicals from industrial wastewater before discharging to the environment.

Toluidine blue (TB) has been used in a number of industrial processes such as the solar and photovoltaic cells [10], inks and toners [11], recording materials [12], paints [13], electrorheological materials [14], textiles [15], detergents [16], analytical diagnostics and security needs [17,18]. In these processes significant amount of water being used, so TB gets part of the wastewater in the environment. Different biological, chemical and physical methods were used for the industrial wastewater treatment. For example, chemical oxidation, electrochemical treatment, liquid–liquid extraction [7], oxidation–ozonation, adsorption, coagulation–flocculation, biological treatment and membrane processes [2]. Among these, adsorption was the simple and cost-effective method but generate solid waste. However, once a dye adsorbed efficiently onto an adsorbent then it may be easy to regenerate the dye and thus can be reused. Activated carbon (AC) has been used as an adsorbent for the removal of dyes, color and taste due to its better adsorption capacity. Mostly, wastewater, vegetable oils and animal oils were treated with AC to remove color, odor, taste and other undesired impurities [19]. For, these applications AC was commonly prepared from agricultural residues such as husk, nut shell, wood, peat, saw dust, lignite, coal, bones, fruit pits, charcoal, waste of paper mills and synthetic fibers. Thus, AC can be a useful material for the removal of TB from aqueous solution.

In this study, the activated carbon from olive pits (ACops) were prepared by chemical activation subsequently with phosphoric acid (H_3PO_4) and potassium hydroxide (KOH) followed by carbonization at 280°C. The prepared adsorbent was characterized using physical techniques and utilized for the removal of TB from aqueous medium under optimal experimental conditions. The batch and fixed bed study of the adsorbent suggest that ACop can be a significant adsorbent for the removal of TB from wastewater.

2. Materials and methods

2.1. Adsorbate

o-Toluidine blue (CAS number; 92-31-9, color index number 52040; $C_{15}H_{16}ClN_3S$, molecular weight; 305.83 g/mol and λ_{max} = 630–635 nm, Sigma-Aldrich) was obtained from a local chemical trader in Pakistan.

2.2. Preparation of adsorbent

Table 1 summarizes the conditions which involve in the preparation of ACop. Briefly, the olive stones were washed, dried and finely crushed. The crushed sample was soaked in a 300 mL of H_3PO_4 (50%) solution for 24 h. The acid activated sample was then treated with 500 mL of KOH (0.5 M) solution. The sample was washed with distilled water until neutralized pH and then carbonized at 280°C on a ramp of 0.5°C/min and maintained at peak temperature for 2 h under nitrogen flow. The sample was cooled to room temperature, crushed and stored in an air tight bottle.

2.3. Characterization

Morphology of the ACop was studied by scanning electron microscopy (SEM, JSM 5910, Jeol, Japan). The X-ray diffraction (XRD) pattern was determined by X-ray diffractometer (JDX-3532, Jeol, Japan) with an X-ray source of Cu Kα (l = 1.5418 Å) at voltage: 20–40 kV, current: 2.5–30 mA and 2θ = 10°–80°. The Brunauer–Emmett–Teller (BET) surface area was analyzed by surface area and pore size analyzer (NOVA2200e, Quantachrome, USA), under nitrogen flow. Fourier transform infrared spectroscopy (FTIR) analysis was performed on Shimadzu, IR Prestige 21, FTIR-8400S, employing diffuse reflectance accessory [DRS-8000A]. The resolution of spectra was 4 cm^{-1} with 50 accumulations in the range of 4,000–500 cm^{-1}.

Table 1
Conditions for preparation of ACop

Precursor	Olive pit
Chemical treatment	H_3PO_4 (50 wt%), KOH (0.5 M)
Carbonization temperature (°C)	280
Before impregnation (w/g)	40
After impregnation (w/g)	29
After heat treatment (w/g)	14.6
Bulk density (g/L)	0.99
% loss (w/g)	63.5

2.4. Batch study

Solutions of desired concentrations were prepared by dissolving TB in deionized water. ACop and TB solutions were loaded into flask and placed in a shaker at desired temperature for specific duration. After experimental run, the adsorption slurry was filtered. The adsorbate concentration in the filtrate was measured by UV-1800 (UV–visible spectrophotometer). The total dye adsorbed in percentage per gram of adsorbent y was determined by Eq. (1), where x_i is the initial concentration of TB solution and x_f is the final concentration of TB solution while w is the adsorbent weight.

$$y = \frac{(x_i - x_f)}{w} \times 100 \quad (1)$$

2.5. Fixed bed column study

In the fixed bed study, a column was packed with ACop. The internal diameter of column was 1.5 cm and height of packed material was 12 cm. The solution (20 mg/L) was allowed to flow under gravity. The final concentration of the solution was determined by UV spectrophotometer.

3. Results and discussion

3.1. Characterization

The SEM images presented in Fig. 1 show the surface morphology of ACop with different magnifications. SEM images reveal the presence of all types of pores on ACop. The macropores are larger in size and considered as the part of external surface of ACop while the measure of micropores and mesopores are given in Table 2, which are responsible for better adsorption of TB on ACop. The pores having width <2 nm are referred as micropores while pores having

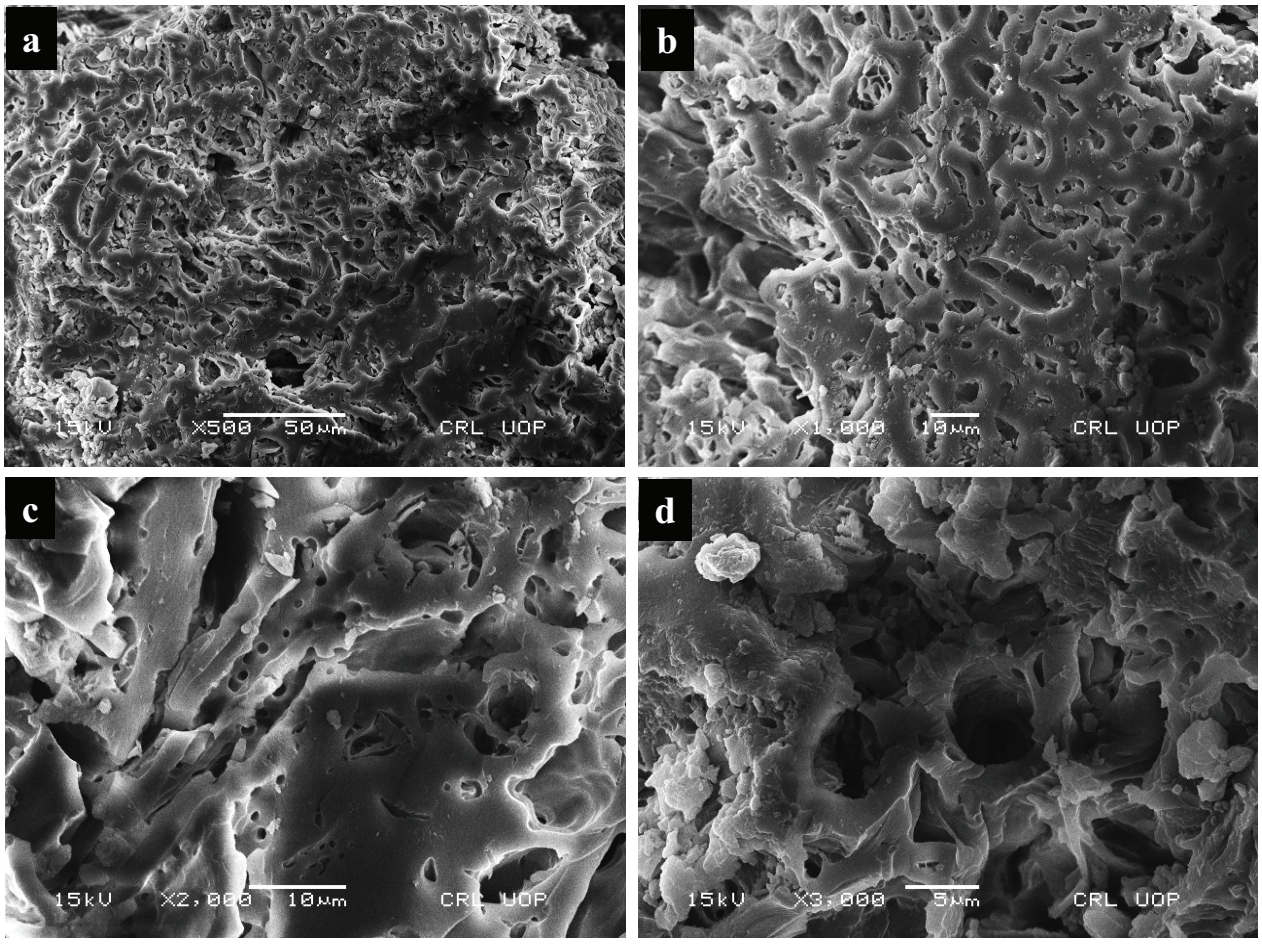

Fig. 1. SEM images of ACop with magnification of (a) 500×, (b) 1,000×, (c) 2,000×, and (d) 3,000×.

Table 2
Pore structure parameters of ACop

Activated carbon	Olive pits
BET surface area (m^2/g)	1,209
Total volume (cc/g)	0.78
Volume of micropores (cc/g)	0.48
Volume of mesopores (cc/g)	0.3

width from 2 to 50 nm are considered as mesopores according to IUPAC nomenclature. In order to find the effect of activation on surface area the olive pit without H_3PO_4 and KOH activation was directly subjected to carbonization at 280°C. The surface area of 180 m^2/g was observed suggested that the activation before carbonization significantly increases the surface area of ACop and thus can enhance the efficiency of the adsorbent. Yakout et al. [20] prepared ACop with activation of H_3PO_4 at different concentrations such as 60, 70 and 80 wt% followed by carbonization at 500°C. The observed surface areas were 257, 779 and 1,218 m^2/g with 60, 70 and 80 wt% H_3PO_4, respectively. In the present study, with 50 wt% of H_3PO_4 and 280°C carbonization surface area of 1,209 m^2/g were achieved. This high surface area may be due to the H_3PO_4 activation followed by KOH (0.5 M) treatment. Redondo et al. [21] synthesized ACop in alkali media KOH followed by carbonization at 700°C. They observed the surface area of 1,815 m^2/g suggested that KOH significantly enhances the surface area of ACop. Thus, we have achieved comparatively large surface area at low carbonization temperature because the acid activation produced channels on the ACop surface whereas the subsequent KOH treatment may functionalized the acid activated channels.

Fig. 2 shows the XRD pattern of ACop. No peaks were observed which suggest the amorphous nature of the ACop. Earlier study reports the similar XRD pattern with no distinctive peak of AC [22].

Figs. 3 shows the FTIR spectra of ACop, treated with H_3PO_4 (50%) and ACop after TB adsorption. Broad peak at 3,420–3,444 cm^{-1} indicates the presence of OH group and water vapors. Further peaks at 2,921 and 2,855 cm^{-1} and 1,450 cm^{-1} show aliphatic C–H stretching in –C–H– and –CH– deformation, respectively. Peaks at 885, 840 and 775 cm^{-1} confirm the deformation of C–H in different substituted benzene ring. The band at 1,700 cm^{-1} refers to C=O stretching vibration of carbonyl groups. In ACop, C–C vibrational band at 1,600–1,580 cm^{-1} was attributed to aromatic ring. As the ACop was treated with H_3PO_4, so the peak at 1,190–1,200 cm^{-1} indicates the presence of (P=O) to O–C stretching vibration (P–O–C hydrogen bonded in aromatic) and also POOH.

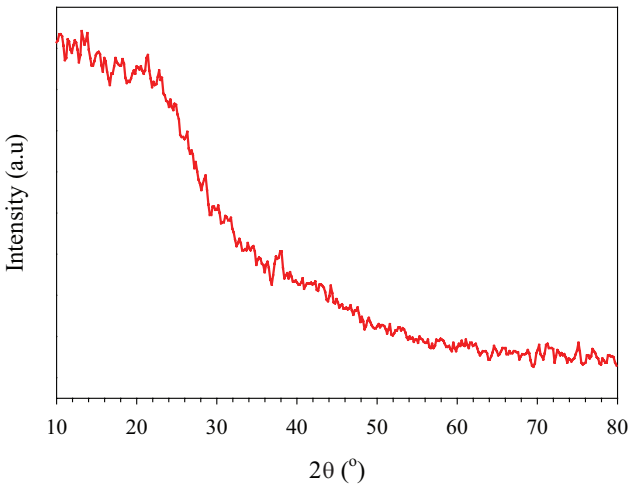

Fig. 2. XRD diffraction pattern of ACop.

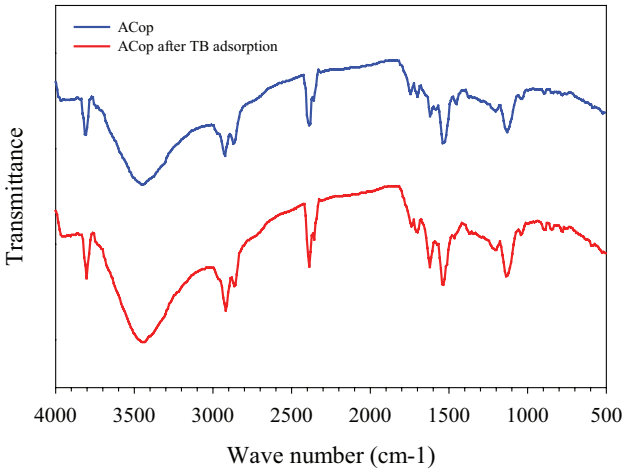

Fig. 3. FTIR spectra of ACop and ACop after TB adsorption.

The symmetrical vibration of P–O–P chain and ionized linkage of P–O– was indicated at 1,100 cm^{-1}.

3.2. Effect of various parameters on percentage removal of TB

The initial pH value of the adsorbate solution is one of the important parameter in adsorption of an ionic species such as cationic TB. The changes in pH value affect the charged density of both adsorbent and adsorbate. Fig. 4 shows the removal of TB (%) at different pHs = 2.5–9.5 at initial dye concentration of 20 mg/L, amount of ACop = 0.5 g, temperature = 298 K, time = 30 min and stirring speed = 250 rpm. The adsorption of TB increased with an increase in pH reached maximum removal of 93 % at pH = 9.5. At acidic pH the low adsorption may be due to the competitive accumulation of protons (H^+) on the adsorbent surface as reported elsewhere [23]. The increase in TB adsorption onto ACop at high pHs was due to electrostatic interaction of oppositely charged ACop and TB at high pH. The TB has two pK_a values of 2.4 and 11.6 [24]. Above these values the TB exhibits cationic

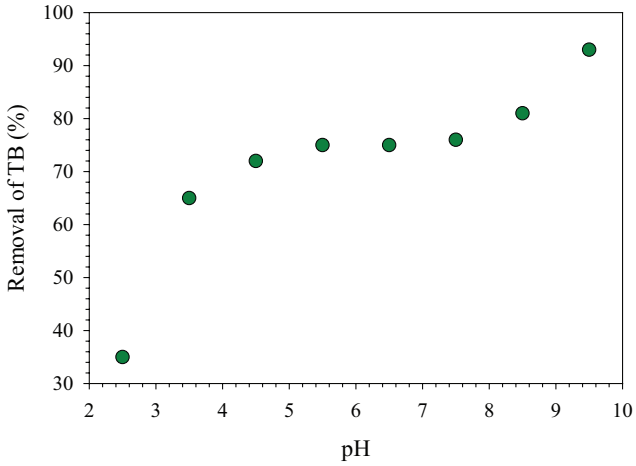

Fig. 4. Removal of TB with ACop as a function of pH.

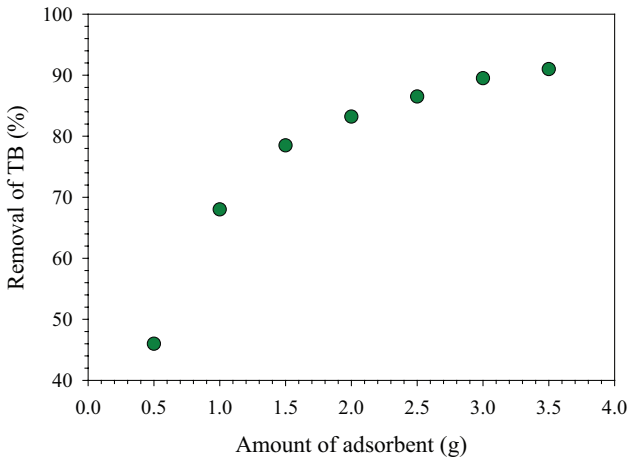

Fig. 5. Removal of TB as a function of amount of ACop.

charges while the ACop has anionic groups on the surface due to acid treatment followed by KOH activation. Thus, at high pH the cationic charged density of TB increases results in high adsorption on the adsorbent surface. Alpat et al. [25], Dogan and Alkan [26] obtained similar enhancement of cationic dyes with increasing pH. In this study, the TB removal was carried at initial solution pH = 7.5 for further experiments or otherwise specified.

To investigate the effect of ACop loading on the adsorption of TB, a series of experiments were carried out with different amount of ACop ranging from 0.5 to 3.5 g while values of other variables were constant; dye concentration (20 mg/L), stirring speed = 250 rpm, pH = 7.5 and contact time = 30 min, as shown in Fig. 5. The percentage removal increased with an increase in ACop dose. This trend was attributed to the ACop surface area and accessibility of more absorption sites, afterward the surface area was proportional to the adsorbent mass in the solution [7].

Fig. 6 shows the adsorption of TB onto ACop as a function of initial dye concentration and time at experimental conditions temperature = 298 K, pH = 7.5, shaking speed

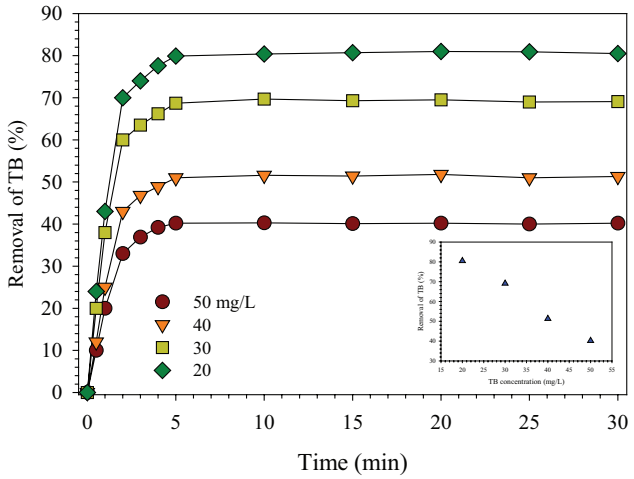

Fig. 6. Adsorption of TB onto ACop at different concentrations.

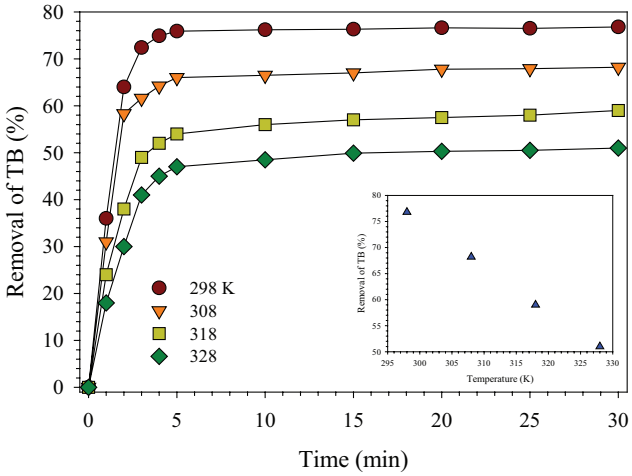

Fig. 7. TB adsorption onto ACop at different temperature.

= 250 rpm and amount of ACop = 0.5 g. Adsorption of TB increased as the time progressed until equilibrium reached at time = 5 min. Moreover, the system achieved equilibrium by further increase in time this may be due to the defined mass transfer of TB molecule from the bulk solution to the outer surface of ACop [27,28]. The percentage removal decreased with increased in concentration of TB. The percentage removal always decreases with increase in initial dye concentration because the high amount of initial dye concentration contains large number of dye molecules and thus the given adsorbent surface occupy with the dye. And thus the amount of dye molecules adsorbed per gram of the ACop was increased with an increase in initial dye concentration.

3.3. Thermodynamic parameters

Fig. 7 shows the effect of temperature on the removal of TB on ACop. The percentage removal of TB decreased from 93% to 49%. This decrease was attributed to the weakening of the interaction of active sites of ACop with TB. The thermodynamic parameters reflect the exothermic adsorption of TB onto ACop, as measured from $\Delta G°$, $\Delta H°$ and $\Delta S°$, using Eqs. (2) and (3):

$$\Delta G° = -RT\ln(K_\circ) \tag{2}$$

$$\ln k_0 = -\frac{\Delta G°}{RT} = \frac{-\Delta H°}{RT} + \frac{\Delta S°}{R} \tag{3}$$

The negative value of $\Delta G° = -10.88$ J suggests that adsorption process was spontaneous, the $\Delta H° = -10.98$ J confirms that the adsorption was exothermic, while $\Delta S° = -3.06 \times 10^{-4}$ indicates that the adsorption of TB on ACop was favorable adsorption process [25].

3.4. Adsorption kinetics

To measure the kinetics of TB adsorption on ACop, the pseudo-first-order and pseudo-second-order kinetics Eqs. (4) and (5) were applied to experimental data:

$$\ln\left(q_e - q_t\right) = \ln q_e - k_i t \tag{4}$$

$$\frac{t}{q_t} = \frac{1}{(k_2 q_e)^2} + \frac{t}{q_e} \tag{5}$$

where q_e is the equilibrium amount of TB and q_t is the amount of TB adsorbed at equilibrium and at any time, t is time, while k_i and k_2 are the rate constant for pseudo–first-order and pseudo-second-order kinetics, respectively. The pseudo-first-order regression showed poor fitting (Fig. 8(a)) while the pseudo-second-order equation has better fitting (Fig. 8(b)) with correlation coefficient value (R^2 = 0.9973) suggest that the TB adsorption onto ACop follow pseudo-second-order kinetics [29].

To determine the rate limiting step in a batch type adsorption process, Weber and Morris [30,31] model was applied to data:

$$q_t = k_i t^{0.5} + C \tag{6}$$

where q_t is the adsorbed amount of TB in mg/g, k_i is the diffusion coefficient value in mg/(g min$^{1/2}$) and t is the time in min. According to Eq. (6), the curve of q_t vs. $t^{0.5}$ should be straight passing over the origin, if the intraparticle diffusion is the rate limiting step, but in Fig. 9 the plot is typically divided into the region with initial smooth curve complied by a linear plot which reveal that diffusion via pores is not a rate limiting step but boundary control layer was also required in the adsorption process.

The most important part of the study was to elucidate the adsorption isotherm for TB adsorption on ACop. The common isotherms for adsorption such as Langmuir, Freundlich and Temkin were investigated for TB adsorption on ACop [32–34]. According to the Langmuir adsorption kinetic, adsorption occur at specific homogenous sites on the adsorbent that are all energetically equivalent.

The Langmuir equation can be linearly written as:

$$\frac{C_e}{q_e} = \frac{1}{q_{\max} b} + \frac{C_e}{q_{\max}} \tag{7}$$

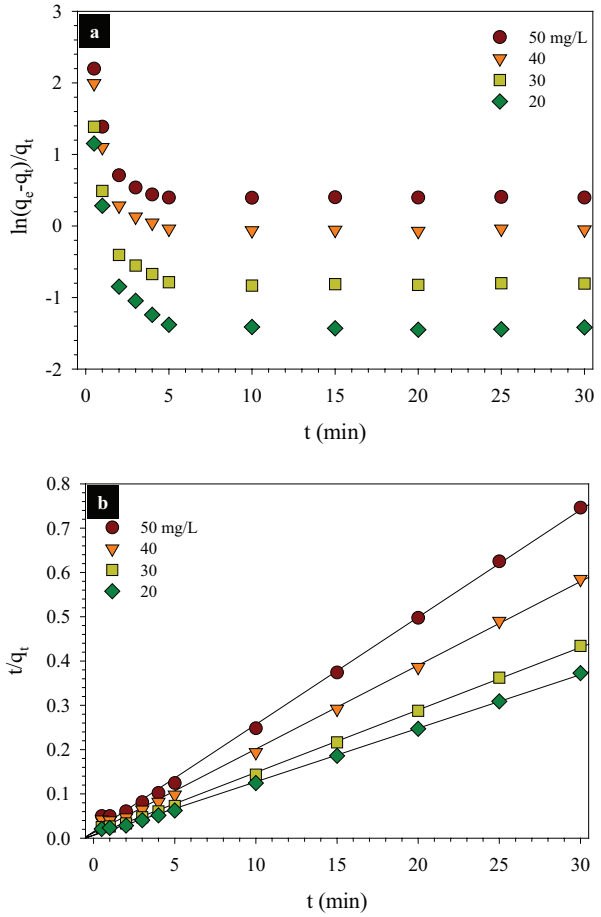

Fig. 8. (a) Pseudo-first-order and (b) pseudo-second-order kinetics of TB adsorption on ACop.

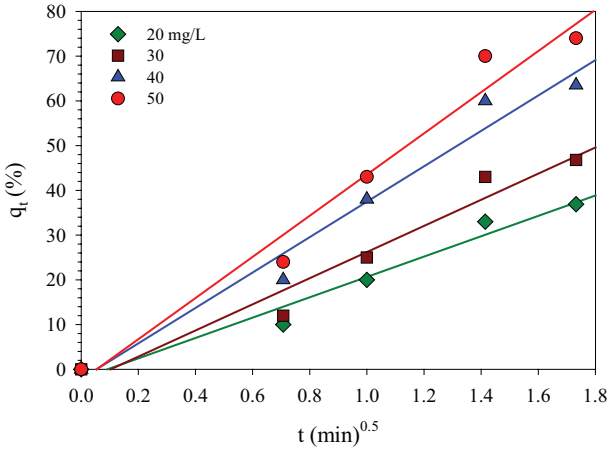

Fig. 9. Plot for the intraparticle diffusion of TB adsorption on ACop.

where q_e is the total adsorbed amount of TB per unit mass of ACop at equilibrium, C_e is the final concentration of TB in a solution at equilibrium, q_{max} is the maximum adsorption at monolayer capacity on ACop and b is the adsorption constant. The favorability of adsorption mechanism is shown by dimensionless equilibrium parameter as follows:

$$R_L = \frac{1}{(1+bC_i)} \tag{8}$$

where C_i is the initial concentration of TB in solution. The value of R_L shows isotherm types, either ($0 < R_L < 1$) favorable, ($R_L > 1$) unfavorable, ($R_L = 1$) linear or ($R_L = 0$) which is irreversible. In this study, the R_L value was observe less than one and greater than zero and confirmed that the adsorption of TB is favorable on ACop.

The Freundlich equation was employed to examine the experimental data for the explanation of heterogeneity of the system, the equation is as follows:

$$\ln q_e = \ln K_F + \frac{1}{n}\ln C_e \tag{9}$$

where K_F is Freundlich constant associated with adsorption process such as adsorption capacity and intensity, respectively. Accordingly, the adsorption data were also subjected to Temkin adsorption isotherm, the linear form of this equation can be written as:

$$q_e = k\ln A + k\ln C_e \tag{10}$$

where k is Temkin binding energy isotherm constant, while A is Temkin isotherm constant. On the basis of R^2 value, the Langmuir model provide a fit at $R^2 = 0.92$ (Fig. 10(a)), smaller than the regression values for Freundlich at $R^2 = 0.95$ (Fig. 10(b)) and Temkin showed best fit at $R^2 = 0.99$ (Fig. 10(c)) adsorption isotherms, respectively. These data confirms the monolayer adsorption followed by multilayers formations.

3.5. Fixed bed column study

In the fixed bed column study, it was observed that the maximum amount of dye was charged to column. In the recent study, the effect of inlet flow rate, height of bed, initial concentration was not investigated. Although the column study gives a clue that AC prepared from olive pit can be used efficiently for the removal of TB from textile industries effluent.

3.6. Fractal analysis

The equation is given as:

$$\ln q_e = \text{constant} - \frac{1}{n}\ln(\ln C_e) \tag{11}$$

$$D_s = 3 - \left(\frac{1}{n}\right) \tag{12}$$

where D is the fractal dimension, C_e is the TB concentration at equilibrium, q_e is the adsorption capacity at equilibrium.

Frenkel–Halsey–Hill plot was constructed for the adsorption of TB on the surface of ACop as presented in Fig. 10(d).

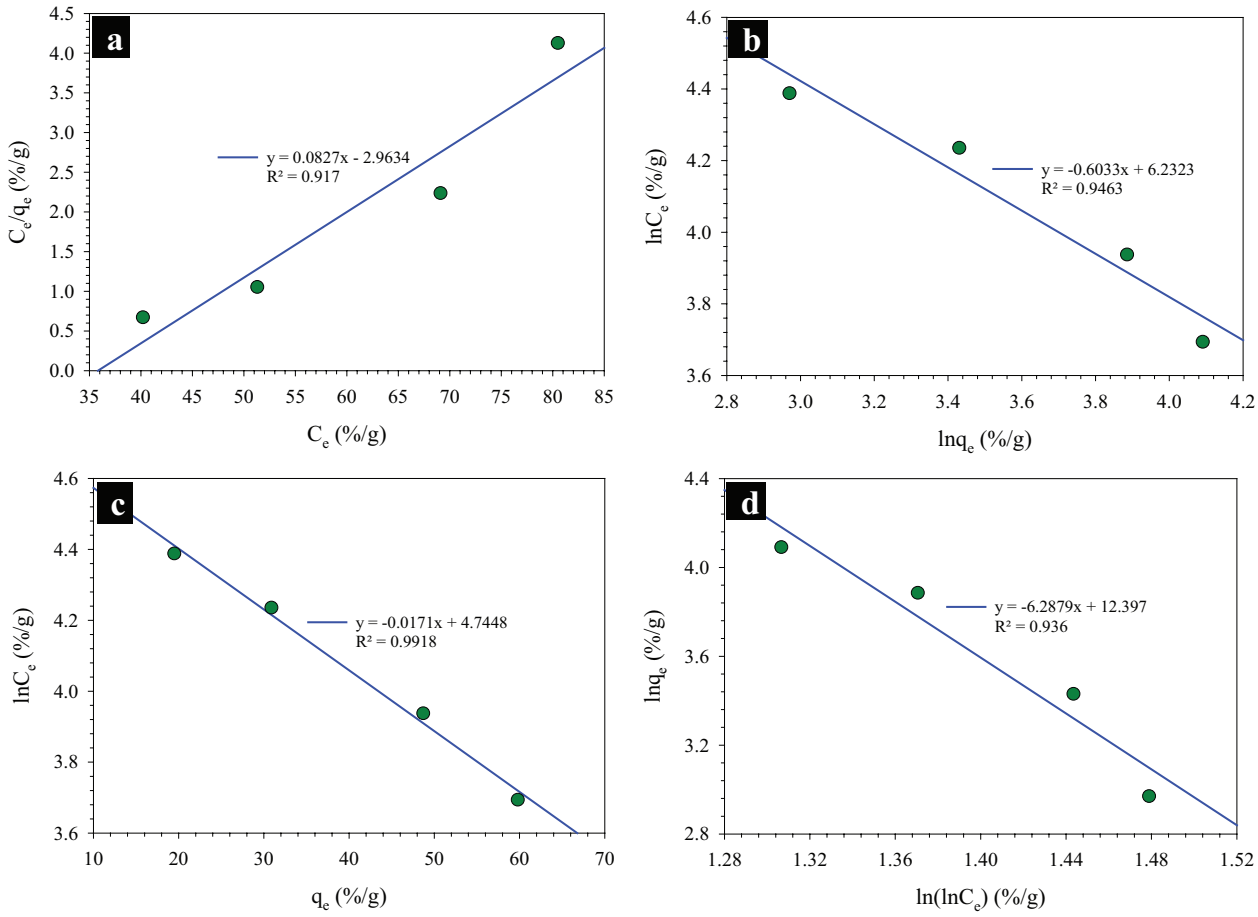

Fig. 10. Adsorption isotherms (a) Langmuir, (b) Freundlich, (c) Temkin curves of TB on ACop; and (d) fractal analysis of ACop.

The value of fractal dimension fall as 2.93 while the regression value is $R^2 = 0.999$. The value of fractal dimension (2.93) gives the description about the heterogeneity of the surface, structural and geometric properties of the surface and porous nature [35]. The value of fractal dimension ≥ 3 represents irregular, rough and porous structure of AC while the value of fractal dimension near to 2, suggests the regular, smooth and nonporous surface of AC [20]. In the present study, *D* value is near to 3 which mean that the surface of ACop is very rough, irregular and porous in nature.

4. Conclusion

The ACop with surface area 1,209 m^2/g and total pore volume 0.78 cm^3/g was utilized for the eradication of TB from aqueous medium. The fractal analysis revealed that the surface of ACop was porous. The maximum adsorption of TB on ACop was 83% at optimal conditions pH = 7.5, concentration of TB = 20 mg/L, dose of adsorbent = 3.5 g/L, time = 5 min and temperature = 298 K. The adsorption of TB on ACop followed pseudo-second-order kinetics with regression value of ($R^2 = 0.99$) and proceeds with Temkin adsorption isotherm ($R^2 = 0.99$). Fixed bed column studies show that ACop was a potent adsorbent material for TB adsorption from the aqueous medium.

Acknowledgment

The authors greatly acknowledge to Higher Education Commission of Pakistan, University of Malakand and Pakistan Science Foundation for financial assistance.

Conflict of interest

This is regarding the publication of this paper, the author declare no conflict of interest.

References

[1] M.A. Rauf, S.M. Qadri, S. Ashraf, K.M. Al-Mansoori, Adsorption studies of Toluidine Blue from aqueous solutions onto gypsum, Chem. Eng. J., 150 (2009) 90–95.
[2] C. Hessel, C. Allegre, M. Maisseu, F. Charbit, P. Moulin, Guidelines and legislation for dye house effluents, J. Environ. Manage., 83 (2007) 171–180.
[3] G. Akkaya, İ. Uzun, F. Güzel, Kinetics of the adsorption of reactive dyes by chitin, Dyes Pigm., 73 (2007) 168–177.
[4] D.M. Lewis, Coloration in the next century, Rev. Prog. Color., 29 (1999) 23–28.
[5] N.F. Cardoso, E.C. Lima, T. Calvete, I.S. Pinto, C.V. Amavisca, T.H.M. Fernandes, R.B. Pinto, W.S. Alencar, Application of aqai stalks as biosorbents for the removal of the Dyes Reactive Black 5 and Reactive Orange 16 from aqueous solution, J. Chem. Eng. Data, 56 (2011) 1857–1868.

[6] N.F. Cardoso, E.C. Lima, I.S. Pinto, C.V. Amavisca, B. Royer, R.B. Pinto, W.S. Alencar, S.F.P. Pereira, Application of cupuassu shell as biosorbent for the removal of textile dyes from aqueous solution, J. Environ. Manage., 92 (2011) 1237–1247.
[7] D. Özer, G. Dursun, A. Özer, Methylene blue adsorption from aqueous solution by dehydrated peanut hull, J. Hazard. Mater., 144 (2007) 171–179.
[8] N.F. Cardoso, E.C. Lima, B. Royer, M.V. Bach, G.L. Dotto, L.A.A. Pinto, T. Calvete, Comparison of *Spirulina platensis* microalgae and commercial activated carbon as adsorbents for the removal of Reactive Red 120 dye from aqueous effluents, J. Hazard. Mater., 241–242 (2012) 146–153.
[9] D.S. Brookstein, Factors associated with textile pattern dermatitis caused by contact allergy to dyes, finishes, foams, and preservatives, Dermatol. Clin., 27 (2009) 309–322.
[10] K.M. Gangotri, C. Lal, Use of mixed dyes in photogalvanic cells for solar energy conversion and storage: EDTA-methylene blue and thionine system, Proc. Inst. Mech. Eng. Part A, 219 (2005) 315–320.
[11] R. Baur, H.T. Macholdt, U. Nickel, L. Unverdorben, C. Wille, Preparation of Azo Colorants in Microreactors and Their Use in Electrophotographic Toners and Developers, Powder Coatings, Ink Jet Inks and Electronic Medias, Google Patents (US 20030083410 A1), 2006.
[12] A.A. Lauber, M.L. Souma, Use of toluidine blue for documentation of traumatic intercourse, Obstet. Gynecol., 60 (1982) 644–648.
[13] D.A. Castle, Pigment analysis in the forensic examination of paints. II. Analysis of motor vehicle paint pigments by chemical tests, J. Forensic Sci. Soc., 22 (1982) 179–186.
[14] C. Hu, Y. Li, Y. Kong, Y. Ding, Preparation of poly(*o*-toluidine)/nano ZnO/epoxy composite coating and evaluation of its corrosion resistance properties, Synth. Met., 214 (2016) 62–70.
[15] S.H. Lin, C.M. Lin, Treatment of textile waste effluents by ozonation and chemical coagulation, Water Res., 27 (1993) 1743–1748.
[16] K. Ramalingam, M.H. Ravindranath, Histochemical significance of green metachromasia to Toluidine blue, Histochemie, 24 (1970) 322–327.
[17] M. Strong, C.W. Vaughan, J. Incze, Toluidine blue in diagnosis of cancer of the larynx, Arch. Otolaryngol., 91 (1970) 515–519.
[18] A.L. Giles, C.W. Chung, C. Kommineni, Dermal carcinogenicity study by mouse-skin painting with 2,4-toluenediamine alone or in representative hair dye formulations, J. Toxicol. Environ. Health, 1 (1976) 433–440.
[19] P.A. Carneiro, G.A. Umbuzeiro, D.P. Oliveira, M.V.B. Zanoni, Assessment of water contamination caused by a mutagenic textile effluent/dyehouse effluent bearing disperse dyes, J. Hazard. Mater., 174 (2010) 694–699.
[20] S. Yakout, G.S. El-Deen, Characterization of activated carbon prepared by phosphoric acid activation of olive stones, Arabian J. Chem., 9 (2011) S1155–S1162.
[21] E. Redondo, J. Carretero-González, E. Goikolea, J. Ségalini, R. Mysyk, Effect of pore texture on performance of activated carbon supercapacitor electrodes derived from olive pits, Electrochim. Acta, 160 (2015) 178–184.
[22] M. Zieliński, R. Wojcieszak, S. Monteverdi, M. Mercy, M.M. Bettahar, Hydrogen storage on nickel catalysts supported on amorphous activated carbon, Catal. Commun., 6 (2005) 777–783.
[23] T.S.Y. Choong, T.N. Wong, T.G. Chuah, A. Idris, Film-pore-concentration-dependent surface diffusion model for the adsorption of dye onto palm kernel shell activated carbon, J. Colloid Interface Sci., 301 (2006) 436–440.
[24] H.A. Mohammad Salim, S.A. Mohammad Salih, Photodegradation study of Toluidine Blue dye in aqueous solution using magnesium oxide as a photocatalyst, Int. J. Chem., 7 (2015) 143–149.
[25] S.K. Alpat, Ö. Özbayrak, Ş. Alpat, H. Akçay, The adsorption kinetics and removal of cationic dye, Toluidine Blue O, from aqueous solution with Turkish zeolite, J. Hazard. Mater., 151 (2008) 213–220.
[26] M. Dogan, M. Alkan, Adsorption kinetics of methyl violet onto perlite, Chemosphere, 50 (2003) 517–528.
[27] R. Lafi, S. Rezma, A. Hafiane, Removal of toluidine blue from aqueous solution using orange peel waste (OPW), Desalin. Wat. Treat., 56 (2015) 2754–2765.
[28] S. Chakraborty, S. Chowdhury, P. Das Saha, Adsorption of Crystal Violet from aqueous solution onto NaOH-modified rice husk, Carbohydr. Polym., 86 (2011) 1533–1541.
[29] S.K. Behera, J.-H. Kim, X. Guo, H.-S. Park, Adsorption equilibrium and kinetics of polyvinyl alcohol from aqueous solution on powdered activated carbon, J. Hazard. Mater., 153 (2008) 1207–1214.
[30] M.A. Rauf, S.B. Bukallah, F.A. Hamour, A.S. Nasir, Adsorption of dyes from aqueous solutions onto sand and their kinetic behavior, Chem. Eng. J., 137 (2008) 238–243.
[31] W.J. Weber, J.C. Morris, Kinetics of adsorption on carbon from solution, J. Sanit. Eng. Div., 89 (1963) 31–60.
[32] I. Langmuir, The constitution and fundamental properties of solids and liquids. Part I. Solids, J. Am. Chem. Soc., 38 (1916) 2221–2295.
[33] H.M.F. Freundlich, Over the adsorption in solution, J. Phys. Chem., 57 (1906) 385–471.
[34] M.J. Temkin, V. Pyzhev, Recent modifications to Langmuir isotherms, Acta Physiochim. URSS, 12 (1940) 217–222.
[35] S.-I. Pyun, C.-K. Rhee, An investigation of fractal characteristics of mesoporous carbon electrodes with various pore structures, Electrochim. Acta, 49 (2004) 4171–4180.